

## Propagating Beam Frame: A Novel Formulation for Local Inverse Scattering

Ram Tuvi<sup>(1)</sup>, Ehud Heyman<sup>(1)</sup>, and Timor Melamed<sup>(2)</sup>

(1) School of Electrical Engineering, Tel Aviv University, Israel. ramtuvi@post.tau.ac.il, heyman@tau.ac.il

(2) Department of Electrical and Computer Engineering, Ben-Gurion University of the Negev, Israel. timormel@bgu.ac.il

### Abstract

We present a novel strategy for tomographic inverse scattering using beam-waves processing. The theory utilizes a discrete phase-space set of beam waves, which constitutes an overcomplete frame everywhere in space, and thus can be considered as a local alternative to the conventional plane-wave or Green's function expansion sets used in the conventional theory. Specifically, we consider an ultra wide band (UWB) inversion scheme that is formulated either in the multi-frequency domain or in the short-pulse time domain. Accordingly, the processing is performed using either a phase-space set of isodiffracting Gaussian beams (ID-GB), or a set of isodiffracting pulsed beam (ID-PB).

### 1 Introduction and Problem Description

We consider local tomographic inversion of weak scatterers using beam-wave processing instead of the conventional Green's function or plane wave inversion schemes where beam-waves are used for both local phase-space processing of the data and for back-propagation and local reconstruction of the object. Tomographic inversion can be performed using either angular diversity or frequency diversity of the data [1]; In this paper, we demonstrate the beam approach for UWB data that is expressed either in the multi-frequency domain or in the short-pulse domain.

Referring to Fig. 1(a), we consider a lossless, non-dispersive medium with wavespeed  $v(\mathbf{r})$  in a 3D coordinate frame, which is embedded in a uniform medium  $v_0$ . The medium is characterized by the “object function”

$$O(\mathbf{r}) = n^2(\mathbf{r}) - 1, \quad n(\mathbf{r}) = v_0/v(\mathbf{r}) = \text{refractive index.} \quad (1)$$

The medium is located between two planes,  $z = z_1 < 0$  and  $z_2 > 0$ , and it is probed by a linear array of sources located on the  $z = z_1$  plane. The scattered field is measured over the receivers arrays on the  $z_1$  and/or  $z_2$  planes, and is henceforth tagged by the index  $j = 1, 2$ , respectively. The excitations are short pulses whose spectrum is essentially bandlimited according to the desired spatial resolution. The data is organized in a data matrix  $\mathbf{D}$  whose  $pq$  element is the field measured at receiver  $q$  due to a unit excitation at source  $p$ .

### 2 Time-domain diffraction tomography

In the TD-DT, introduced in [2] (see Fig 2), the medium is illuminated by a pulsed plane wave (PPW)  $u^i(\mathbf{r}, t) = f(t - v_0^{-1} \hat{\mathbf{k}}^i \cdot \mathbf{r})$  where  $f(t)$  is a short pulse and the unit vector  $\hat{\mathbf{k}}^i$  defines the wave direction. Under the

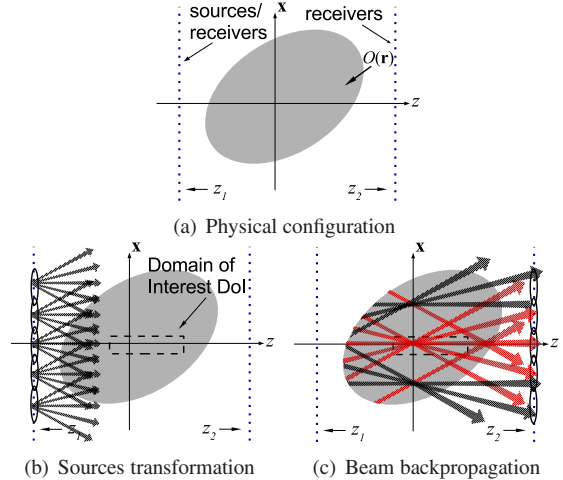


**Figure 1.** Physical configuration and the beam-based inverse scattering: (a) The unknown object  $O(\mathbf{r})$  is located between the measurement planes  $z = z_{1,2}$ . (b) The point-source and point-receiver data is transformed to the beam domain data due to a phase-space set of beam excitations and a phase-space set of beam receivers. (c) Beam-domain back-propagation and reconstruction: Only those beams that pass through the domain of interest (DoI), depicted red, are considered.

Born approximation, the scattered field is related to the Radon transform of  $O(\mathbf{r})$  along the bisector between  $\hat{\mathbf{k}}^i$  and the observation direction [2], as schematized by the red Radon projection plane in the Figure. In the inversion, one calculates the backpropagated field  $u_j^b(\mathbf{r}, t)$  from the data measured on the  $z_j$  plane (see Sec. 4.1), and then calculates the “imaging fields”,  $I_j(\mathbf{r}, t)$ ,

$$-\partial_t^2 I_j(\mathbf{r}, t) = 2v_0 \hat{\mathbf{k}}^i \cdot \nabla u_j^b(\mathbf{r}, t + v_0^{-1} \hat{\mathbf{k}}^i \cdot \mathbf{r}), \quad j = 1, 2. \quad (2)$$

The recontracted object  $\check{O}(\mathbf{r})$  is obtained by setting the *imaging condition*

$$\check{O}(\mathbf{r}) = I_1(\mathbf{r}, t)|_{t=0} + I_2(\mathbf{r}, t)|_{t=0}. \quad (3)$$

### 3 Phase-Space Beam Summation Methods

**3.1 Phase space beam summation method:** For simplicity we present the method in the context of radiation into the half space  $z > 0$  due to a given time-harmonic field distribution  $\hat{u}_0(\mathbf{x})$  in the  $z=0$  plane where we use the coordinate convention  $\mathbf{r} = (\mathbf{x}, z) = (x_1, x_2, z)$  and an over-caret denotes fields with  $e^{-i\omega t}$  harmonic dependence. Originally, in the 1980's, the method has been structured upon a Gabor

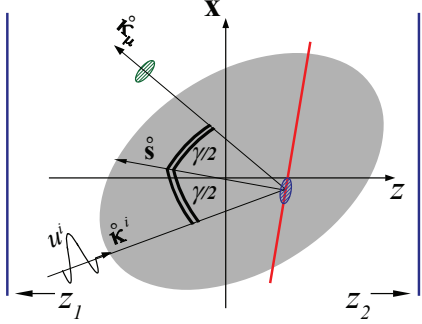


**Figure 2.** Time-domain diffraction tomography. The figure illustrates both the pulsed plane-wave (PPW) formulation of Sec. 2, and the pulsed-beam (PB) formulation of Sec. 4. In the former, the scattered field is related to the Radon transform of  $O(\mathbf{r})$  along the axis  $\hat{s}$  that bisects the angle  $\gamma$  between  $\hat{\mathbf{k}}^i$  and the scattering direction, as schematized by the red projection plane. In the latter, the scattered PB along the  $\mu$  axis (the green ellipses) is related to the Local Radon transform of  $O(\mathbf{r})$  (the blue ellipses) [2].

expansion of  $\hat{u}_0(\mathbf{x})$ , but it has undergone several substantial extensions, and today, following [3], it is structured upon a *windowed Fourier transform (WFT)* frame expansion. The WFT frame set  $\{\hat{\psi}_{\mu}(\mathbf{x})\}$  is defined by

$$\hat{\psi}_{\mu}(\mathbf{x}) = \hat{\psi}(\mathbf{x} - \mathbf{x}_m)e^{ik\xi_n \cdot (\mathbf{x} - \mathbf{x}_m)}, \quad k = \omega/v_0, \quad (4)$$

$\mu = (\mathbf{m}, \mathbf{n}) = ((m_1, m_2), (n_1, n_2)) \in \mathbb{Z}^4$  is an index that tags the frame elements,  $\hat{\psi}(\mathbf{x})$  is a localized “mother window” (typically a Gaussian) and  $(\mathbf{x}_m, \xi_n) = (\mathbf{m}\bar{x}, \mathbf{n}\bar{\xi})$  is a phase-space lattice with  $(\bar{x}, \bar{\xi})$  defining the unit-cell. Anticipating an extension to the time domain we use the normalized spectral variable  $\xi = \mathbf{k}_x/k$ . The frame elements in (4) are centered about the lattice  $(\mathbf{x}_m, \xi_n)$  with the parameters  $(\bar{x}, \bar{\xi})$  chosen to provide an overcomplete coverage of the  $(\mathbf{x}, \mathbf{k}_x)$  phase space in the sense that

$k\bar{x}\bar{\xi} = 2\pi v$ ,  $v < 1$  defines the overcompleteness, (5)  
with  $v \uparrow 1$  defining the critically complete (Gabor) limit.

The aperture field  $\hat{u}_0(\mathbf{x}, \omega)$  can then be expanded as

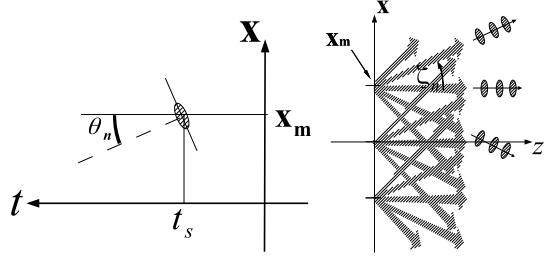
$$\hat{u}_0(\mathbf{x}) = \sum_{\mu} \hat{a}_{\mu} \hat{\psi}_{\mu}(\mathbf{x}), \quad \hat{a}_{\mu} = \langle \hat{u}_0(\mathbf{x}), \hat{\phi}_{\mu}(\mathbf{x}) \rangle, \quad (6)$$

where  $\langle f, g \rangle$  are the conventional  $\mathbb{L}_2$  inner product in  $\mathbf{x}$  and  $\{\hat{\phi}_{\mu}\}$  is the “canonical dual frame,” which has the WFT frame form in (4) with  $\hat{\psi}$  replaced by the “dual window”  $\hat{\phi}(\mathbf{x})$ . In general  $\hat{\phi}$  needs to be calculated numerically for a given  $\hat{\psi}$  and lattice  $(\bar{x}, \bar{\xi})$ , but for a sufficiently overcomplete lattice ( $v \lesssim 1/3$ )  $\hat{\phi}(\mathbf{x}) \propto \hat{\psi}(\mathbf{x})$ , thus simplifying the calculations. In view of the structure of  $\hat{\phi}_{\mu}$ , it follows that  $\hat{a}_{\mu}$  in (6) are WFT of  $\hat{u}_0(\mathbf{x})$  around the lattice points  $(\mathbf{x}_m, \xi_n)$  with respect to the window function  $\hat{\phi}(\mathbf{x})$ .

The radiated field for  $z > 0$  is obtained by propagating the expansion set  $\hat{\psi}_{\mu}(\mathbf{x}, \omega)$  in (6), giving

$$\hat{u}(\mathbf{r}) = \sum_{\mu} a_{\mu} \hat{\Psi}_{\mu}(\mathbf{r}), \quad (7)$$

the “beam propagators”  $\hat{\Psi}_{\mu}$  are the fields radiating  $z > 0$  due to the aperture fields  $\hat{\psi}_{\mu}(\mathbf{x})$  on  $z = 0$ . If  $\hat{\psi}$  is wide on a wavelength scale then  $\hat{\Psi}_{\mu}$  behave like collimated beams whose axes emerge from the points  $\mathbf{x}_m$  in the  $z = 0$  plane in the directions  $(\theta_n, \phi_n)$  such that  $\sin \theta_n (\cos \phi_n, \sin \phi_n) =$



(a) WRT expansion in the data plane (b) The propagated field

**Figure 3.** The PS-PBS method. (a) The WRT in the data domain  $(\mathbf{x}, t)$  is schematized by the small ellipse centered at  $(\mathbf{x}_m, t_s)$  with spectral tilt  $\xi_n$ . (b) The field is expressed as a sum of PB propagators (schematized as small ellipses) that propagate along the beam axes (the dashed arrows).

$\xi_n$  (see dashed arrows in Fig. 3(b)). Propagating beams obtained only for  $|\xi_n| \lesssim 1 - \Delta_{\xi}$  where  $\Delta_{\xi}$  is the spectral width of  $\hat{\psi}$  ( $\Delta_{\xi} \ll 1$  for collimated beams).

**3.2 UWB Phase Space Beam Summation (UWB-PS-BS):** The degree of freedom introduced in (5) has been utilized to formulate two UWB expansion schemes that apply either in the multi-frequency domain [4] or directly in the time domain [5] (Sec. 3.3). The idea is to use *the same beam lattice*  $(\bar{x}, \bar{\xi})$  for all  $\omega$  in the pertinent frequency band  $\Omega = [\omega_{\min}, \omega_{\max}]$ . Following (5), this implies that  $v(\omega) = \omega \frac{v_{\max}}{\omega_{\max}}$  where  $v_{\max} = v(\omega_{\max})$ , so that  $v(\omega) < v_{\max}$  for all  $\omega \in \Omega$ . Following the discussion after (6) we typically choose  $v_{\max} \approx 1/3$  and use the approximation  $\hat{\phi}(\mathbf{x}) \propto \hat{\psi}(\mathbf{x})$  for all  $\omega \in \Omega$ .

Another important ingredient in this theory is the use of the *iso-diffracting Gaussian Beams (ID-GB)* propagators, defined by the mother window

$$\hat{\psi}_{\text{ID}}(\mathbf{x}, \omega) = e^{-k|\mathbf{x}|^2/2b}, \quad (8)$$

where the parameter  $b$  is the *collimation* length of the resulting GB and is taken to be  $\omega$ -independent, hence the ID designation. The ID-GB propagators have many favorable properties, including: (i) They can be tracked analytically in inhomogeneous medium; (ii) Their propagation parameters are  $\omega$ -independent, hence they need to be calculated only once and then used for all  $\omega$ ; (iii) Consequently, they can be expressed explicitly in the time-domain as *iso-diffracting pulsed Beams (ID-PB)* [6], hence the entire expansion can be formulated directly in the time domain [5]. (iv) Finally, choosing  $b = \bar{x}/\bar{\xi}$  provides the *snuggest* expansion for all  $\omega \in \Omega$ , with stable expansion coefficients.

**3.3 Phase-Space Pulsed-Beam Summation (PS-PBS):** As noted after (8), the UWB-PS-BS formulation can be expressed directly in the TD. The theory has been derived in [5] in the context of radiation from a time-dependent aperture distribution  $u_0(\mathbf{x}, t)$ , band limited in  $\Omega$ . It utilizes a new type of frame, termed *windowed Radon transform (WRT)* frame, structured upon a 5D lattice  $(\mathbf{x}_m, \xi_n, t_s) = (\mathbf{m}\bar{x}, \mathbf{n}\bar{\xi}, \bar{t}s)$  in the  $(\mathbf{x}, t)$  domain, where  $\bar{t}$  is the temporal sampling interval satisfying the Nyquist condition and  $(\mu, s) = (\mathbf{m}, \mathbf{n}, s) \in \mathbb{Z}^5$  is an index. We then define the space-time “mother” and “dual” windows via

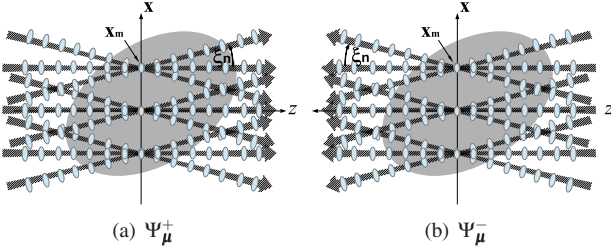


**Figure 4.** The propagating PB frames (a):  $\Psi_{\mu,s}^+$ , and (b):  $\Psi_{\mu,s}^-$ . The individual PB are depicted as small ellipses along the beam axes, for different values of the time index  $s$ .

$\psi(\mathbf{x}, t)$  } =  $\text{Re} \frac{1}{\pi} \int_0^\infty d\omega e^{-i\omega t} \left\{ \hat{f}(\omega) \hat{\psi}(\mathbf{x}, \omega) \right\}$  (9)  
where  $\hat{f}, \hat{g}$  which are introduced to add flexibility to the formulation, are constraint by  $\hat{f}(\omega) \hat{g}^*(\omega) = 1 \forall \omega \in \Omega$  in order to guaranty duality there. The dual WRT frame sets  $\{\psi_{\mu,s}(\mathbf{x}, t)\}$  and  $\{\varphi_{\mu,s}(\mathbf{x}, t)\}$  are obtained by inverting the WFT frame sets  $\{\hat{f}(\omega) \hat{\psi}_\mu(\mathbf{x}, \omega)\}$  and  $\{\hat{g}(\omega) \hat{\varphi}_\mu(\mathbf{x}, \omega)\}$  of (4) to the time coordinate  $t - t_s$ , giving

$$\psi_{\mu,s}(\mathbf{x}, t) = \psi(\mathbf{x} - \mathbf{x}_m, t - t_s - v_0^{-1} \xi_n \cdot (\mathbf{x} - \mathbf{x}_m)), \quad (10)$$

with a similar expression for  $\varphi_{\mu,s}$ . These frame elements are localized about the space-time point  $(\mathbf{x}_m, t_s)$  with spectral slant  $\xi_n$  (Fig. 3(a)). The sets  $\psi_{\mu,s}$  and  $\varphi_{\mu,s}$  constitute dual frame sets in the  $(\mathbf{x}, t)$  domain for in the Hilbert space  $\mathbb{L}_2^\Omega$  of band limited functions [5].

The aperture distribution  $u_0(\mathbf{x}, t) \in \mathbb{L}_2^\Omega$  is expanded as

$$u_0(\mathbf{x}, t) = \sum_{\mu,p} a_{\mu,s} \psi_{\mu,s}(\mathbf{x}, t), \quad (11a)$$

$$a_{\mu,s} = \bar{t} \langle u_0(\mathbf{x}, t), \varphi_{\mu,s}(\mathbf{x}, t) \rangle_{(\mathbf{x}, t)} \quad (11b)$$

where the inner product in (11b) implies projection of  $u_0(\mathbf{x}, t)$  onto  $\varphi_{\mu,s}(\mathbf{x}, t)$ . In view of the slanted structure of  $\varphi_{\mu,s}$  (see (10) and Fig. 3(a)), this operation is regarded as a WRT of  $u_0$  in the 3D  $(\mathbf{x}, t)$  domain.

Equation (11a) can be propagated to  $z > 0$  giving

$$u(\mathbf{r}, t) = \sum_{\mu,s} a_{\mu,s} \Psi_{\mu,s}(\mathbf{r}, t), \quad (12)$$

The PB propagators  $\Psi_{\mu,s}(\mathbf{r}, t)$  are the field at  $z > 0$  due to the aperture distribution  $\psi_{\mu,s}(\mathbf{x}, t)$  at  $z = 0$  (explicit expressions are given in [5]). As schematized in Fig. 3(b), the representation in (12) expresses the radiated field as a sum of PB emerging from the aperture at a discrete set of initiation points, directions and times.

**3.4 The beam-frame (BF) concept:** The BF extends the PS-BS and PS-PBS methods from the  $z = 0$  plane into any  $z = \text{const}$  plane in the propagation domain [7]. We consider the sets of forward and backward propagating beams  $\{\hat{\Psi}_\mu(\mathbf{r})\}_{\mu_p}$  depicted as arrows in Fig. 4, where  $\mu_p$  tags the subset of “propagating beams” such that  $|\mathbf{n}\xi| < 1$ .

**The BF Theorem [7]:** The set of forward propagating beams  $\{\hat{\Psi}_\mu(\mathbf{r})\}_{\mu_p}$  constitutes a frame at any  $z = \text{const}$  plane over the Hilbert subspace  $\mathbb{L}_p(\mathbf{x})$ , with  $\{\hat{\Phi}_\mu(\mathbf{r})\}_{\mu_p}$  being the “canonical dual frame”. Here  $\mathbb{L}_p(\mathbf{x})$  is the Hilbert space of functions with propagating spectrum only

(i.e., their spectrum vanishes for  $|\xi| > 1$ ), and  $\hat{\Phi}_\mu(\mathbf{r})$  are the beam-waves corresponding to  $\hat{\varphi}_\mu(\mathbf{x})$  at  $z = 0$  (choosing parameters as discussed in Sec. 3.2,  $\hat{\Phi}_\mu^+(\mathbf{r})$  are  $\propto \hat{\Psi}_\mu^+(\mathbf{r})$ ). The beam expansion is given by (7), but the expansion coefficients can be calculated from the data at any given  $z = \text{const}$  plane via the inner product in (6) with  $\hat{\varphi}_\mu(\mathbf{x})$  replaced by  $\hat{\Phi}_\mu^+(\mathbf{r})$ . Note that the BF is structured upon the beam skeleton in the phase space, and reduces to the conventional WFT frame at the  $z = 0$  plane, which is structured upon a Cartesian phase-space lattice. The same formulation applies also for backward propagating fields using the beam sets  $\{\hat{\Psi}_\mu^-(\mathbf{r}), \hat{\Phi}_\mu^-(\mathbf{r})\}_{\mu_p}$ .

In view of the UWB construction of the BF outlined in Sec. 3.2, it has been subsequently extended to the time domain [8]. It has been shown that the forward/backward propagating ID-PB’s  $\{\Psi_{\mu,s}^\pm(\mathbf{r}, t)\}_{(\mu_p, s)}$ , schematized by the ellipses in Fig. 4, constitute frames at any  $z = \text{const}$  plane over the Hilbert subspace  $\mathbb{L}_p^\Omega(\mathbf{x}, t)$  of functions band-limited in  $\Omega$ , with  $\{\Phi_{\mu,s}^\pm(\mathbf{r}, t)\}_{(\mu_p, s)}$  being the canonical dual frames. These pulsed-beam frames (PBF) are an extension of the WRT into any  $z = \text{const}$  plane. The PB expansion of the field is given, again, by (12) where the expansion coefficients can be calculated from the data at any given  $z = \text{const}$  plane via the inner product in (11b) with  $\varphi_{\mu,s}(\mathbf{x}, t)$  replaced by  $\Phi_{\mu,s}^\pm(\mathbf{r}, t)$ .

The BF Theorem implies that the BF formulation can be used to decompose any volume source distribution, real or induced, and thus provide an alternative to the conventional plane wave spectrum approach, in the frequency or time domains. This approach has been used in [7] and in subsequent publications in the context of wave propagation through rough media. In the present paper we use it to formulate a new local inverse scattering scheme.

## 4 Beam-based TD-DT

**4.1 The backpropagated field:** We now use the BF concept introduced in Sec. 3.4 to address the TD-DT problem put forward in Sec. 2. As noted there, the reconstructed  $O(\mathbf{r})$  is calculated from the backpropagated field via (2)–(3). Given the scattering data  $u_{1,2}(\mathbf{x}, t)$  on the  $z_{1,2}$  planes, the PB summation representation of the backpropagated fields  $u_{1,2}^b$  is given by

$$u_{1,2}^b(\mathbf{r}, t) = \sum_{\mu,s} a_{\mu,s}^{(1,2)} \Psi_{\mu,s}^\mp(\mathbf{r}, t) \quad (13a)$$

$$a_{\mu,s}^{(1,2)} = \bar{t} \langle u_{1,2}(\mathbf{x}, t), \Phi_{\mu,s}^\mp \rangle_{(\mathbf{x}, t)} \quad (13b)$$

where the indices 1,2 are associated with the backward/forward propagators, respectively, identified by the superscripts  $\mp$ . Expression (13b) is a generalization of (11b) using the dual beam frames  $\Phi_{\mu,s}^\mp$  instead of  $\varphi_{\mu,s}$ . Expression (13a) is a generalization of (12). Note that we calculate  $u_{1,2}^b$  in the target domain, i.e., for  $z \in [z_1, z_2]$ .

**4.2 The beam-domain data-object relation within the Born approximation:** An analytic model for the beam domain data  $a_{\mu,s}^{(1,2)}$  can be obtained by using the Born approximation for the data and then calculating the coefficients as noted in Sec. 4.1. The result is

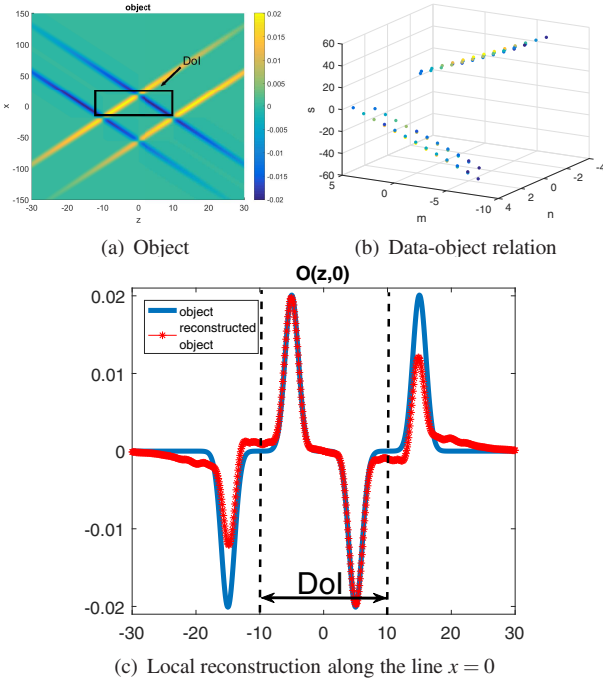


**Figure 5.** Numerical example: (a) The object. (b) Distribution of the dominant  $a_{\mu,s}^{(1)}$  coefficients in the discrete  $(m,n,s)$  phase space. The magnitude of the coefficients is tagged by the color code from brightest to darkest. (c) Reconstruction along the DoI line  $x = 0$ ,  $z \in [-10, 10]$ . Note the excellent reconstructions inside the DoI whereas outside the DoI, the reconstructed  $O$  practically vanishes due to the beam localization.

$$a_{\mu,s}^{(1,2)} = \frac{\bar{t}}{2 \cos \theta_n v_0} \langle O(\mathbf{r}), \dot{\Phi}_{\mu,s}^{\mp}(\mathbf{r}, t) \rangle \Big|_{t=v_0^{-1} \kappa^i \cdot \mathbf{r}} \quad (14)$$

where  $\dot{\Phi} \stackrel{\text{def}}{=} \partial_t \Phi$  and  $\cos \theta_n = \sqrt{1 - |\xi_n|}$ . The operation in (14) is a projection of  $O(\mathbf{r})$  on the window  $\dot{\Phi}_{\mu,s}^{\mp}(\mathbf{r}, t - v_0^{-1} \kappa^i \cdot \mathbf{r})$ , schematized by the red ellipses in Fig. 2. This sampling window is orthogonal to the direction  $\hat{s}$  that bisects the angle between the direction of incidence  $\hat{\kappa}^i$  and the scattered PB direction  $\hat{\kappa}_\mu$ , while its location along this axis is determined by the time parameter  $s$ . This operation is therefore identified as a local Radon transform of  $O(\mathbf{r})$ . The validity of this local model for the data is verified by the results in Fig. 5(b).

**4.3 Local reconstruction of  $O(\mathbf{r})$ :** Inserting (13a) into (2), the imaging fields are given as a sum of PB propagators

$$I_{1,2}(\mathbf{r}, t) = -4 \sum_{\mu,s} a_{\mu,s}^{(1,2)} \cos^2 \frac{\gamma}{2} \partial_t^{-1} \Psi_{\mu,s}^{\mp}(\mathbf{r}, t + v_0^{-1} \kappa^i \cdot \mathbf{r}). \quad (15)$$

**4.4 Numerical example:** We consider a 2D problem with  $\mathbf{r} = (x, z)$ .  $O(\mathbf{r})$  consists of 4 Gaussians, shifted and tilted at  $\pm 15^\circ$  as illustrated in Fig. 5(a). The domain of interest (DoI), marked by a black rectangular, is  $x \in [-20, 20]$  and  $z \in [-10, 10]$ . The medium is probed by a normally incident PPW, and the scattered data is measured only on the  $z_1 = -100$  plane.

Fig. 5(b) depicts the beam domain data  $a_{\mu,s}^{(1)}$ , calculated from the scattering data  $u_1(\mathbf{x}, t)$  via (13b). The figure

depicts these coefficients in the discrete  $(m, n, s)$  domain, where the magnitude of the coefficients is tagged by the color code from brightest to darkest. Only the largest coefficients are shown. This figure verifies the theoretical model for the coefficients in (14). As explained there, the coefficients constitute a local Radon transform sampling of  $O(\mathbf{r})$  and therefore are localized in regions where  $\theta_n \simeq \pm 30^\circ$ , representing the bistatic reflections from the direction of incidence (here  $\theta^i = 0$ ) to  $\theta_n$ . The  $(m, s)$  coordinates correspond to the  $(x, z)$  coordinates of the reflection points.

Finally, the reconstructed  $\tilde{O}(\mathbf{r})$  inside the DoI is calculated via (3) using the PB backpropagation in (15) where only those PB's passing through the DoI are retained in the  $(\mu, s)$  summation. The resulting  $\tilde{O}(\mathbf{r})$ , depicted in red in Fig. 5(c), agrees very well with the original  $O(\mathbf{r})$  in blue, and practically vanishes outside the DoI although  $O(\mathbf{r})$  does not vanish there.

### Acknowledgment

This research is supported by the Israeli Science Foundation (ISF), Grant No. 412/15.

### References

- [1] A.J. Devaney, *Mathematical Foundations of Imaging, Tomography and Wavefield Inversion*, Cambridge University Press, 2012.
- [2] T. Melamed, Y. Ehrlich, and E. Heyman, “Short-pulse inversion of inhomogeneous media: A time-domain diffraction tomography,” *Inverse Problems*, vol. 12, pp. 977–993, 1996.
- [3] D. Lugar and C. Letrou, “Alternative to Gabor’s representation of plane aperture radiation,” *Electronics Letters*, vol. 34, pp. 2286–2287, 1998.
- [4] A. Shlivinski, E. Heyman, A. Boag, and C. Letrou, “A phase-space beam summation formulation for ultra wideband radiation,” *IEEE Trans. Antennas Propagat.*, vol. 52, pp. 2042–2056, 2004.
- [5] A. Shlivinski, E. Heyman, and A. Boag, “A pulsed beam summation formulation for short pulse radiation based on windowed Radon transform (WRT) frames,” *IEEE Trans. Antennas Propagat.*, vol. 53, pp. 3030–3048, 2005.
- [6] E. Heyman and L.B. Felsen, “Gaussian beam and pulsed-beam dynamics: complex-source and complex-spectrum formulations within and beyond paraxial asymptotics,” *J. Opt. Soc. Am. A*, vol. 18, pp. 1588–1611, 2001.
- [7] M. Leibovich and E. Heyman, “Beam domain formulation for wave propagation in weakly rough Media,” *The XXXI General Assembly of URSI*, Beijing, China, August 2014.
- [8] R. Tuvi, T. Melamed, and E. Heyman, “Propagating beam frame: A novel formulation for time-dependent radiation and scattering,” *Electromagnetic Theory Symposium (EMTS)*, Espoo, Finland, August 2016, pp. 169–172.